Materials and Structures (2020) 53:126
https://doi.org/10.1617/s11527-020-01561-1

ORIGINAL ARTICLE

Autogenous and drying shrinkage of mortars based on Portland and calcium sulfoaluminate cements

Davide Sirtoli · Mateusz Wyrzykowski · Paolo Riva · Pietro Lura

Received: 8 May 2020 / Accepted: 21 September 2020 / Published online: 30 September 2020

Abstract Calcium sulfoaluminate (CSA) cement can be used as an alternative binder in concrete, partially or fully replacing ordinary Portland cement. While CSA cement considerably accelerates the mechanical properties development, the rapid evolution of the microstructure together with the high water demand cause rapid and large volume changes at early ages. As volume changes may lead to early-age cracking, measures to reduce them may be required In this paper, autogenous and drying shrinkage are studied in mortars prepared with Portland cement, CSA cement or a 50/50 blend as binder. Very fast self-desiccation and high autogenous shrinkage of the CSA-based mortar were observed compared to the mortar made with Portland cement. On the other hand, the early-age volume changes can be limited if a blend of the two cements is used. The blended system revealed a bi-modal trend in the evolution of self-desiccation and autogenous shrinkage, in which the initial fast self-desiccation and shrinkage enter the dormant phase after the first couple of days and again start after about 28 days.

Keywords CSA · OPC/CSA blends · Early age · Volume changes

1 Introduction

With a yearly production of 4 billion tons [1], ordinary Portland cement (OPC) is essential for the construction industry but it also represents an ecological issue due to the high energy consumption and large amounts of CO_2 emitted during its production [2, 3]. Partial solutions to alleviate this problem are the use of supplementary cementitious materials blended with OPC [4] and the use of alternative fuels in cement kilns [5]. As about 60% of the CO_2 emissions in Portland cement production come from the calcination of limestone, another more radical alternative is to modify the cement chemistry, in particular towards cements that are to a lesser degree based on CaO [3].

Calcium sulfoaluminate cement (CSA) emits less CO_2 compared to OPC thanks to both the use of raw

Electronic supplementary material The online version of this article (https://doi.org/10.1617/s11527-020-01561-1) contains supplementary material, which is available to authorized users.

D. Sirtoli (✉) · P. Riva
Department of Engineering, University of Bergamo, Viale Marconi 5, 24044 Dalmine, Italy
e-mail: davide.sirtoli@unibg.it

D. Sirtoli · M. Wyrzykowski · P. Lura
Empa, Swiss Federal Laboratories for Materials Science and Technology, Dübendorf, Switzerland

P. Lura
Institute for Building Materials, ETH Zurich, Zurich, Switzerland

materials containing less limestone and the lower temperature of clinkerization [6]. The key-component of this material is ye'elimite, a calcium sulfoaluminate mineral ($C_4A_3\overline{S}$); other phases are belite (C_2S), ferrite (C_4AF), mayenite ($C_{12}A_7$) and anhydrite [7]. During hydration, ettringite (AFt) is formed from ye'elimite, lime and sulphates, the latter of particular importance for the hydration kinetics [7, 8]. Monosulphate (AFm) and aluminum hydroxide (AH_3) begin to form instead of ettringite in case of lack of sulphate, while in blends of CSA and OPC other hydration products such as C–S–H, strätlingite or hydrogarnet may additionally form [9]. Considering the blended system CSA/OPC [10, 11], it was observed that the precipitation of AFt during the hydration process of CSA is the main process responsible for the characteristic properties of the hardening material, such as rapid setting, early-age strength development [12] and shrinkage compensation [8, 12]. Moreover, in these blends OPC reaction becomes evident after a few days [11]. Some other factors were also found to influence the expansive behavior of CSA-based systems [13], such as the type and amount of calcium sulfate [14, 15] and the amount of OPC in the blends [11].

Nowadays, due to the high cost of the CSA raw materials and the insufficient characterization of CSA-based concrete for structural applications, CSA cement is mainly used as expansive agent to compensate shrinkage of OPC concrete and generate expansion and self-stress [16–19] and, in few cases, in the production of self-levelling screeds [20, 21], sealing mortar for road works [22] and high performance concrete with rapid strength development at early age [21, 23].

Between the 1970s and the 1990s, an important research and production effort targeted at both CSA and CSA-belite cements took place in the People's Republic of China. Even though the amounts of CSA produced yearly were comparatively low, several Chinese standards were written based on this experience. According to a summary about this period [24], CSA cement found specialized application in small/medium precast concrete shapes, heavily pre-stressed concrete elements, casting in cold environments, high performance concrete, mass and impermeable concrete, glass-fiber reinforced concrete and as expansive admixture. The key feature in all these applications was the rapid hardening behavior and the subsequent fast development of mechanical properties in concrete made with CSA cement.

While the rapid hardening and the rapid gain of mechanical properties has been a main reason of the renewed interest in CSA cements in recent years, it can lead to uncontrolled volume changes (both expansion and shrinkage) and cracking at early ages. Therefore, it becomes crucial to investigate its deformation behavior from the first moment when a solid skeleton is able to resist stresses develops (setting time). Moreover, both sealed and drying condition are of interest, inasmuch they represent the conditions in the field before and after the operation of demolding. While some information is available on shrinkage and expansion of CSA cement paste under water curing condition, little has been published on volume stability of concrete mixtures in realistic conditions (e.g., sealed curing or early drying). Limiting or at least predicting the shrinkage of concrete structures is essential in view of reducing the risk of restrained shrinkage cracking at early ages [25, 26].

Following Jensen and Hansen [27], autogenous deformation is defined as "the bulk deformation of a closed, isothermal, cementitious material system not subjected to external forces". It is related with the drop of the internal RH (self-desiccation) in the pores within the concrete due to the water consumption during hydration. The related pore fluid pressure represents the main driving force for autogenous shrinkage. According to [27], self-desiccation and autogenous shrinkage occur when there is less water in the system than required by the stoichiometric water demand of the cement. While the stoichiometric water-to cement ratio (w/c) for an ordinary Portland cement is around 0.40–0.42, for CSA cement it can be as high as 0.75 [28] (depending on the composition). The mixtures investigated in the present study all have an under-stoichiometric w/c, necessary for reaching high mechanical properties and good workability; this at the same time means that they tend to experience self-desiccation in sealed conditions. Generally, autogenous conditions in concrete structures are typical in elements not yet demolded or in structures with large cross-section, in which the outer layers dry out by losing moisture to the environment, while the inner part, far away from the drying front, undergoes only self-desiccation. The same logic applies to the case when concrete is water cured on the surfaces but its interior still experiences self-desiccation. The latter

difference in moisture state across a concrete element is particularly important in low w/c concretes, due to their low permeability [29]. Autogenous shrinkage typically develops in a matter of days to weeks. As reported by many authors (e.g., [26, 30, 31]) autogenous shrinkage in concrete must be limited because it may induce microcracking or macrocracking and compromise the durability.

After the onset of external drying, drying shrinkage takes place. Depending on the relative humidity (RH) of the environment, the strain pattern changes, especially the total amount developed [26]. Drying shrinkage may lead to macrocracking due to shrinkage gradients that induce internal stresses (self-restraint) [32]. Both drying and autogenous shrinkage can also cause macrocracking due to the presence of external restraints, which leads to the buildup of restraint stresses.

The aim of this study is to investigate the volume changes of mortars containing CSA cement from the moment of setting under different environmental conditions, covering a range of ambient RH. Mortar mixtures were chosen as model for high-performance concrete, saving a considerable amount of material and equipment costs due to their smaller mixture volume required to prepare the samples for the tests. At the same time, the studied shrinkage is amplified in the mortars compared to concrete, due to the larger volume of cement paste (the shrinking phase) in the mortars. The volume changes and the mechanical properties of three different mortar mixtures were investigated: a pure calcium sulfoaluminate cement mixture (CSA), a Portland CEM II A-LL 42.5 *R* mixture (PC) and a blend of the two at a mass ratio of 50/50 (MIX). While the two main mixtures are CSA and MIX, PC is used as a reference to compare their performance to a well-known material.

2 Materials and methods

2.1 Materials

Three different mortar mixtures were made with (1) pure calcium sulfoaluminate cement (i.tech ALI CEM GREEN® by Italcementi), (2) a limestone Portland cement CEM II A-LL 42.5 R, and (3) a blend of the two (50/50 mass ratio) cements. The mortars were called CSA, PC and MIX respectively. These mortar mixtures are based on concrete mixes employed in previous studies [33, 34], in which concrete mixtures were designed with the same strength class C50/60 at 28 days and a workability slump class of at least S4 after 45 min from water addition. These concrete mixtures all corresponded to high-performance concrete with low w/c. In the mortars prepared for the present study, the aggregates (maximum particles size of 2 mm, density of 2700 kg/m^3, water absorption 0.62 mass % according to EN 1097-6) made up nominally 55% of the total volume. This means that the volumetric paste content was nominally the same for all mixes. The main components of the CSA cement (density 2900 kg/m^3) were (by mass %, measured with QXRD by the producer): ye'elimite 53.0, anhydrite 18.7, bredigite 10.7, C_2S 7.7. The main components of the limestone Portland cement (density 3010 kg/m^3) were[1]: C_3S 55.4, C_2S 9.3, C_3A 3.3, C_4AF 9.7 and calcite 12.4. More details on the materials used here can be found in [34]. Three different admixtures were added in different amounts to achieve the mix design aims. A polycarboxylate-based admixture was used as superplasticizer in liquid form in all mortars. Citric acid as hydration retarder and lithium carbonate as set inductor, both as powders, were added to the mortars containing CSA cement. The mixtures proportions are reported in Table 1.

2.2 Mixing procedure

1/3 of the mixing water was added to wet the aggregates. After two minutes, the cement was added and the mixing operation started, while gradually adding the remaining water. Admixtures were added after 90, 135 and 180 s for superplasticizer, retarder and set inductor, respectively. After 210 s, the mixing operation was stopped to mix manually and next mechanical mixing was resumed for further 30 s. In total, the mixing operation required four minutes.

2.3 Compressive strength, flexural strength and static modulus of elasticity

Measurements of static Young's modulus, compressive strength and flexural strength were performed at

[1] According to cement chemistry notation: C_3S–$3CaO{\cdot}SiO_2$, C_2S–$2CaO{\cdot}SiO_2$, C_3A–$3CaO{\cdot}Al_2O_3$, C_4AF–$3CaO{\cdot}Al_2O_3{\cdot}Fe_2O_3$.

Table 1 Mixture proportions of the three chosen materials in (kg/m^3 of mortar)

	MIX	CSA	PC
CEM II-LL 42.5R	288	–	660
ALICEM Green	288	542	–
Sand 0–1	829	829	829
Sand 1–2	658	658	658
SP (% on binder)	1	0.4	1.4
Retarder (% on binder)	0.5	0.4	–
Accelerator (% on binder)	0.2	0.1	–
Water	259	271	231
w/b	0.45	0.5	0.35

1, 3, 7 and 28 days following the EN 196 standard for compressive and flexural strength and the EN 12,390-13:2013 [35] for the static Young's modulus. Measurements were carried out on prismatic samples of dimensions 40 × 40 × 160 mm^3 (duplicate samples for Young's modulus and triplicate samples for strength). The samples were produced pouring the mold in two layers and vibrating for 10 s after each pour. Once the upper surface was rectified, the samples were stored in a chamber at 20 °C and 95% RH for 24 h covered with a glass plate to prevent moisture loss. After this initial period, the samples were demolded, sealed with plastic sheet and stored in a chamber at 20 °C and 95% RH until the day of testing.

2.4 Isothermal calorimetry

A conduction calorimeter (Thermometric TAM Air) was used to determine the rate of heat liberation due to cement hydration during the first week. After the normal mixing procedure, approximately 9 g of mortar were weighed into a flask that was then capped and placed into the calorimeter. Data were plotted after normalizing for the cement mass in the sample. Due to the external mixing, the very early thermal response (the first peak upon water addition) of the samples could not be measured; the results are presented starting from 1 h from mixing. The total heat of hydration after one week was determined by integration of the heat flux curve between the first minimum, after the initial peak, and 7 days.

2.5 Gravimetric sorption measurements

Gravimetric measurements of changes in water content due to RH variation at constant temperature (sorption isotherms) were performed using a Dynamic Vapor Sorption analyzer (DVS). The device allows continuous monitoring of the mass changes in samples exposed to changing RH by means of a high-precision microbalance of accuracy 10 μg to which the sample holder is suspended. The material in the chamber is exposed to changing RH in a controlled flow of a mixture of dry nitrogen and water vapor. The RH is controlled with accuracy ± 1% by means of a dew point analyzer and the temperature with accuracy of ± 0.1 °C by means of Peltier elements. Small slices (9 × 9 × 0.5 mm^3) were extracted at the age of 182 days from the inner part of the prismatic samples (dimensions 40 × 40 × 160 mm^3), used previously for shrinkage measurements (one sample for each tested mixture). The initial RH was set at 90%. Thereafter, decreasing steps by 10% RH followed, until reaching a value of 10% RH; subsequently, the RH was stepwise increased back to 95% RH. The equilibrium criterion was set at 0.0010% mass change in 10 min. The reference dry mass for the calculation of the water content was eventually obtained by drying the sample in a flow of dry nitrogen (0% RH) at 40 °C for 30 h at the end of the measurement. Such temperature was chosen in order to accelerate the drying process yet not to cause any chemical decomposition of the hydration products (mainly ettringite [36]).

2.6 Relative humidity

The fresh mortar was poured into sealed plastic containers just after mixing and stored in a chamber at 20 °C and 95% RH. Just before the moment of setting, the sample was enclosed into a hermetic measuring chamber and the test started. The RH evolution was measured with HC2-AW water activity stations by Rotronic. The nominal trueness of the sensors was ± 0.8% RH. The sensors were calibrated with 4 saturated salt solutions with equilibrium RH in the range of 75–98%. The temperature of the measuring chamber was maintained at 20 ± 0.05 °C by means of water circulating in the casing of the measuring chambers connected to a water bath. The readings were logged at 1 min intervals. The presented

results are the average from 3 samples measured at the same time in three different stations. The measurements lasted for 1 week after mixing.

2.7 Setting time

Initial and final set were determined with the Vicat needle test and the final set results were used for zeroing the autogenous shrinkage measurements (see next section). Results are reported as the average of three tests. The needle was released at intervals of 5 min. The final set was considered as the moment in which the needle could not penetrate anymore into the mortar. Usually this method is applied to cement paste; however, in this case it was assumed that the penetration of the needle was not influenced by the aggregates due to their small dimension and the ∅ 1 mm needle adapted for mortars. The measurements were carried out in a temperature-controlled room at 21 ± 0.3 °C and the moisture conditions were controlled applying a stretched food-wrap atop the specimens, guaranteeing sealed condition during the test. The sample had the form of a truncated cone with 75 and 85 mm diameters and 40 mm height enclosed in PVC molds.

2.8 Autogenous strain

Depending on the investigated period, two types of measurements were performed. For the early age shrinkage, an automatic setup was chosen, which acquires data with 1-min intervals by LVDTs. After 24 h, manual measurements were started and continued until 182 days. Specimens undergoing automatic measurements were cast on a vibrating table into corrugated polyethylene molds with about 425 mm length and 30 mm diameter [37]. At approximately 40 min after water addition, the samples were placed on a rigid stainless-steel frame, capable of accommodating six specimens, immersed in a silicone oil bath maintained at 19.8 ± 0.1 °C and data acquisition was started. The measurements were referred to the time of final set obtained by Vicat needle (see Sect. 2.7). The results are expressed as the average of two samples. More information about this automatic setup can be found in [38].

Manual measurements of autogenous deformation were carried out on three prismatic samples of 40 × 40 × 160 mm^3 produced following the same procedure of the compressive strength samples. After demolding, they were sealed with aluminum tape and measured in a metallic frame equipped with a digital deformation transducer in a room conditioned at 20 ± 0.3 °C. Mass measurements were also taken to verify the quality of sealing. Automatic and manual measurements were combined together in order to obtain a complete description of the autogenous shrinkage after setting. The superposition of both measurements from 24 h to 7 days allowed to confirm the reliability of both methods and the possibility of combining them into one representation.

2.9 Drying strain

The samples used in these measurements are of the same kind of the one used for manual autogenous strain measurements, including curing and initial storage. After 24 h from water addition, they were demolded and placed in four distinct chambers with constant temperature of 20 ± 0.1 °C and different RH: 36, 57, 70 and 90% (all ± 3% RH). These different RH levels were chosen to investigate the effect of the external RH on the mortars by measuring strain and mass change. The acquired data were used in combination with the automatic autogenous shrinkage results measured with the corrugated tube from the time of final set until the beginning of drying, in order to have a complete shrinkage set with different moisture conditions. These conditions simulate concrete in real applications, in which demolding is often performed after about 24 h, thereby exposing the structure to the environment. The results reported are the average of three samples with a measuring accuracy of ± 10 μm/m.

3 Results

3.1 Compressive strength, flexural strength and static Young's modulus

Table 2 shows the mechanical properties for the investigated mixtures in terms of compressive strength, flexural strength and static Young's modulus. While the mixtures containing CSA show a faster development of the mechanical properties at early ages (e.g., the compressive strength of CSA is twice that of PC at 1 day), the PC mixture eventually ends up

with higher modulus and strength. While MIX shows similar strength and modulus as CSA at 1 day, the compressive strength develops less at later ages, the elastic modulus is constant after 1 day and the flexural strength shows even a small decrease (less than 10%).

3.2 Isothermal calorimetry

The results of isothermal calorimetry are shown in Fig. 1. No dormant period was evident for CSA, where the acceleration period started just after 1 h from water addition. The main peak was reached after 2 h, followed by a rapid decrease of the rate of heat liberation until the end of the test. In the CSA/Portland cement blend, the acceleration period started at about the same time as the CSA but the rate of heat liberation was lower. Different peaks were recorded in the first 6 h, likely due to the influence of the admixtures on the hydration reactions. The main peak is reached after 4 h and is three times smaller than for the CSA. After about 6 h, the rate of heat liberation gradually decreased. The Portland cement-based mixture showed a completely different evolution in time. The fast hydration observed for both systems containing CSA binder are due to the formation of ettringite in the first hours from water addition, as shown by the TGA results presented in the Supplementary Materials (Fig. S.1). After the first initial peak, there is a dormant period until 8 h, followed by an acceleration period between 8 and 18 h when the main peak is reached. Compared to the CSA, the Portland cement peak is about ten times smaller. At the end of the experiment, all three systems released a similar amount of heat (from 250 J/g for MIX to 280 J/g for PC), see Fig. 1b. It should be stressed that the values of cumulative heat are only approximate and are necessarily underestimated. This is because the mortars were by necessity mixed externally and the integration of the released heat started only from 1 h after water addition, after temperature equilibration in the calorimeter. This most likely led to an underestimation of cumulative heat, especially for the two mixes containing CSA due to their initial fast reaction, whereas it likely affected the results for the PC mix to a negligible extent.

3.3 Gravimetric sorption measurements

The sorption results for the three mixtures are reported in Fig. 2. PC had lower total water content but showed relatively higher water loss (mostly between 50 and 10% RH). CSA and MIX had higher total water content and more gradual desorption. All mortars recovered their moisture content when the RH was ramped up to 95% and showed hysteresis between about 30 and 90% RH.

Table 2 Properties of the three mixtures in terms of setting time, compressive strength, flexural strength and static Young's modulus

	Setting time (min)	Age (days)	Compressive strength (MPa)	Flexural strength (MPa)	Static Young's modulus (GPa)
PC	408	1	26.3 ± 0.3	5.93 ± 0.11	19.1 ± 0.0
		3	55.1 ± 0.1	8.77 ± 0.40	27.3 ± 0.1
		7	62.7 ± 0.5	9.30 ± 0.61	29.9 ± 0.1
		28	70.6 ± 0.4	10.00 ± 1.04	31.5 ± 0.1
CSA	66	1	45.6 ± 0.1	7.10 ± 0.61	24.9 ± 0.1
		3	49.7 ± 0.1	7.40 ± 0.10	25.9 ± 0.3
		7	59.0 ± 1.3	8.73 ± 0.31	28.7 ± 0.1
		28	67.9 ± 0.6	9.00 ± 0.80	31.1 ± 0.1
MIX	84	1	46.7 ± 0.7	7.77 ± 0.15	25.0 ± 0.6
		3	52.6 ± 0.9	7.53 ± 0.32	25.4 ± 0.2
		7	52.3 ± 1.2	7.37 ± 0.21	25.6 ± 0.1
		28	63.0 ± 0.6	7.27 ± 0.15	26.5 ± 0.1

Results are reported as the average of three samples for strength and two samples for Young's modulus with their standard deviation

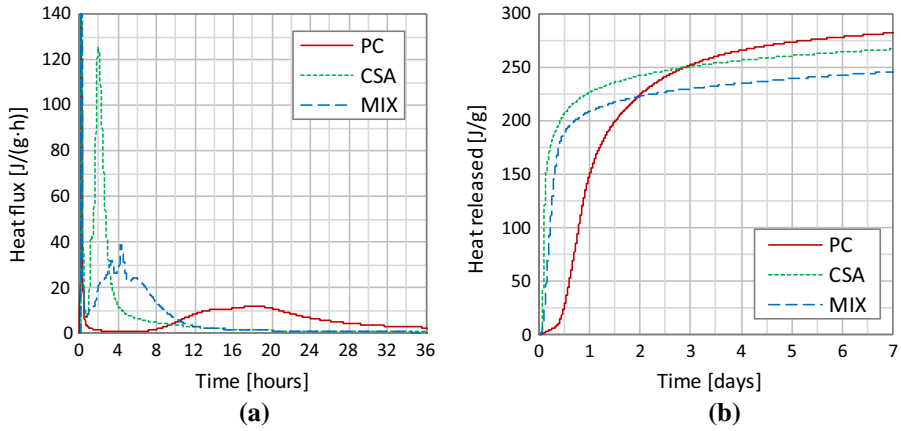

Fig. 1 Isothermal conduction calorimetry for the three investigated mixtures; **a** heat flux in the first 36 h; **b** cumulative heat until 7 days

3.4 Internal RH

Figure 3 shows the internal RH evolution in time in autogenous conditions for the three investigated mortars. The graph reports the mean value in bold lines of the three samples investigated for each mixture, with the standard deviation bands drawn with thinner lines. When self-desiccation in Portland cement based mixtures is studied, this test usually lasts for a couple of weeks. In order to take into account the complex RH evolution of MIX, longer measurements were performed in the systems containing calcium sulfoaluminate cement. PC desiccated only moderately, reaching 92% RH after 14 days, while CSA showed a fast initial drop to 84% RH just after 24 h. MIX behaved in markedly different manner compared to both pure systems. After a RH drop in the first 12 h, similarly to CSA, the rate of RH drop decreased and it reached about 95–96% RH after 3 days. After a period of stability, the RH started decreasing again around 14 days from water addition.

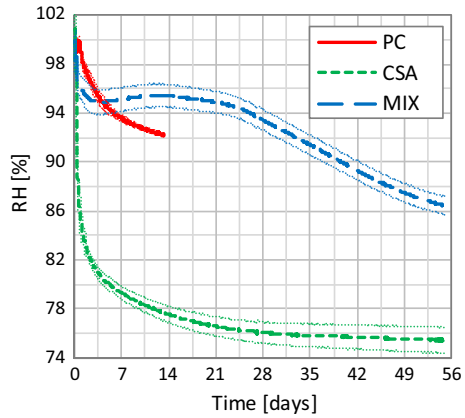

Fig. 3 Relative humidity evolution in autogenous condition for the three investigated mortars

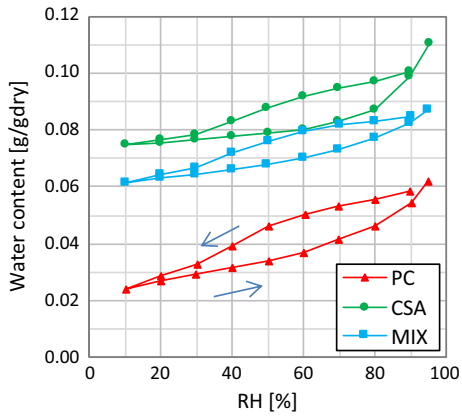

Fig. 2 Sorption isotherms at 20 °C at 182 days for the three investigated mixtures in the range 10–95% RH. The water content was calculated with reference to the dry specimen mass at 0% RH and 40 °C

3.5 Autogenous shrinkage

Figure 4a shows the autogenous deformation results for the three mortars until 24 h. The curves represent the mean value of two samples in bold lines while the standard deviation is drawn as bands with thin lines. PC showed rapid shrinkage for the first 2 h after final set, followed by slight expansion and a substantial plateau (at a total shrinkage value of about 100 μm/m) up to 24 h. CSA showed much faster shrinkage after final set, reaching values around 800 μm/m in the first 30 min; after a discontinuity, the slope started to decrease constantly but at lower late, reaching

1200 µm/m at 24 h. MIX had intermediate behavior, with rapid initial shrinkage close to that of CSA but reaching a plateau just 1 h after set at about 300 µm/m.

From 24 h onwards, strain measurements were taken with the manual setup. Combining the automatic and measuring technique is justified based on the results of the comparison of the two methods presented in detail in the Supplementary Materials, Fig. S.3. These results show that the differences of autogenous shrinkage resolved by the two methods in the period 1–14 days are in the range 20–40 µm/m, hence very low compared to the overall magnitude of shrinkage. Figure 4b shows the overall strain development in autogenous conditions (combining automatic dilatometer and manual readings), from the time of set to 182 days. CSA continues to shrink until 28 days at a higher rate compared to the other two mortars, reaching a value about 1600 µm/m. The strain rate then decreases, adding only 150 µm/m in the next 5 months. PC showed the smallest shrinkage, 350 µm/m at 28 days and only additional 50 µm/m in the next 5 months. MIX had intermediate total shrinkage, with a complex evolution in time. During the first week, a shrinkage of 450 µm/m was measured, followed by a phase with slight expansion until 28 days. Unlike the other mortars, at this stage MIX started a second shrinkage phase with higher shrinkage rate until 70 days, when the rate started to decrease. From 28 days to 6 months, the blended mortar showed the highest autogenous shrinkage, about 250 µm/m.

3.6 Mass change

Figure 5 shows the mass change in time of samples stored at different RH. For all mortars, samples stored at 90% RH had markedly different evolution than in the other environments. After an initial loss of mass during the first days, PC started to adsorb water from the external environment, recovering over time the lost mass. On the contrary, CSA showed a steady mass gain as soon as it was exposed to 90% RH. MIX lost a small amount of water at early age followed by a small gain until 14 days, then moderate loss until 35 days and finally continuous gain until 6 months of age.

At the other RH levels (36, 57 and 70% RH), PC and MIX showed higher mass loss than CSA. Of the three mortars, MIX exhibited the highest mass losses at 70 and 57% RH, while OPC had slightly higher mass loss at 36% RH.

3.7 Drying shrinkage

Figure 6 shows the drying shrinkage evolution of the specimens exposed to drying at different RH from 1 day. These curves are plotted together with the autogenous shrinkage measured with the automatic setup (Fig. 4a) in the first 24 h (before demoulding) to give a complete picture of the total deformations. As expected, for all mortars, the lower the RH the higher the shrinkage. When only the results after 24 h are considered, MIX shrinks much less than the other mortars. For the harshest drying condition (36% RH), MIX reached shrinkage of about 480 µm/m after

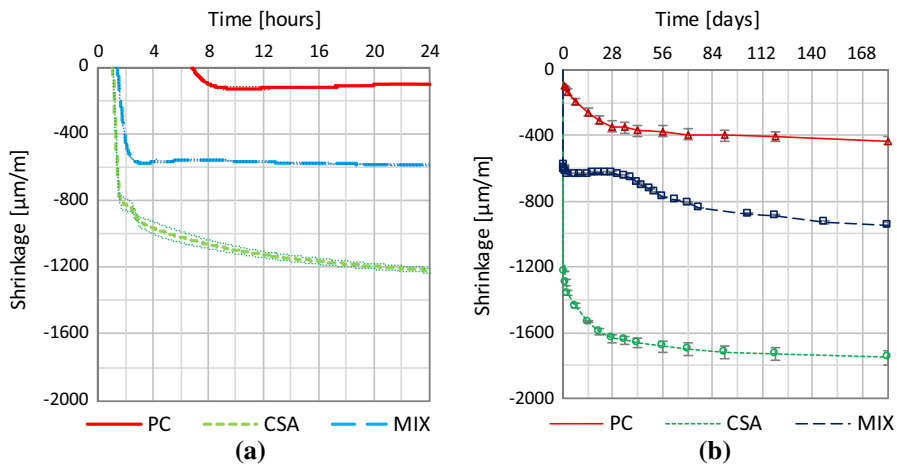

Fig. 4 Autogenous shrinkage evolution; **a** automatic measurements until 24 h; **b** combination of automatic and manual measurements until 182 days

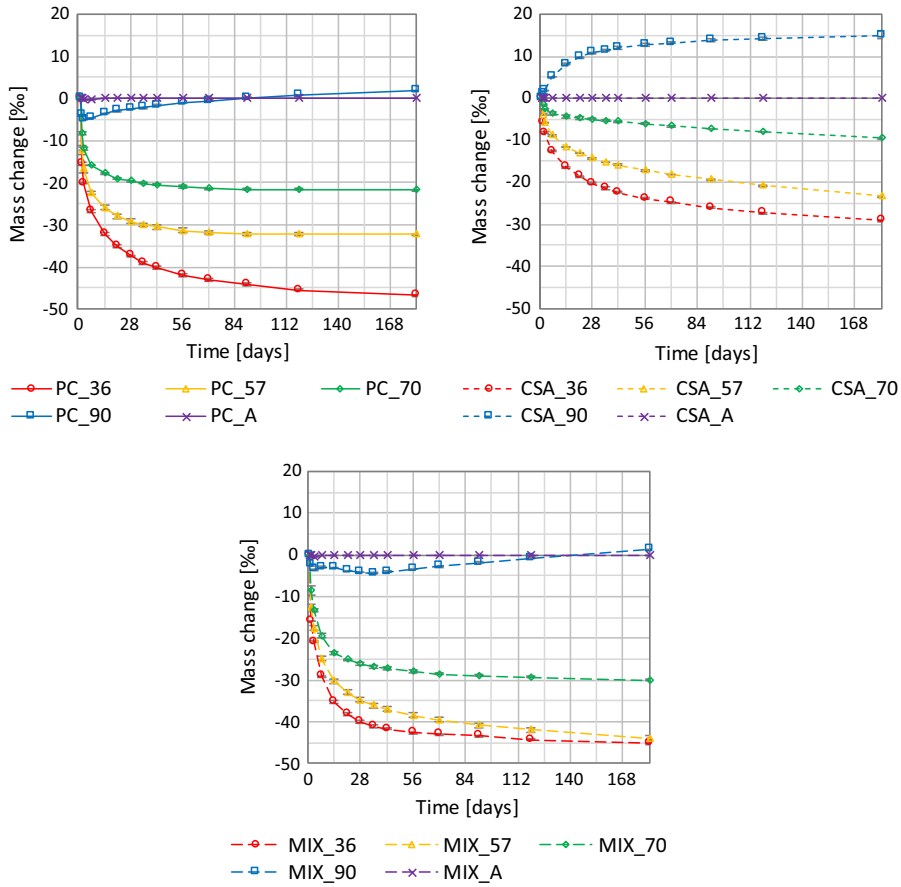

Fig. 5 Mass change evolution (with respect to initial mass) for specimens demolded after 24 h and stored at different RH

180 days, while CSA and PC shrunk 880 µm/m and 1330 µm/m, respectively.

Both CSA and MIX cured at 90% RH started to expand at 7 days from water addition. While CSA continued to expand over time, MIX soon reached a plateau. In PC, the shrinkage at 90% RH is close to the autogenous shrinkage curve, while in CSA it is close to the shrinkage measured at 70% RH. On the other hand, the autogenous shrinkage of MIX is similar to the shrinkage measured at 90% RH in the first 28 days. At this point, a period of increasing shrinkage rate followed, after which the autogenous shrinkage reached values close to the shrinkage at 70% RH.

4 Discussion

The very high autogenous shrinkage strains experienced by the mortars with CSA are due to the w/c of these mixes, which is considerably lower than that necessary for full hydration [28]. This is due to the high bound water content of the CSA cement. The total bound water content is the sum of the chemically bound water and the physically bound water [39]. The sum of these two bound water types corresponds to the minimum w/c necessary for reaching full hydration. If the w/c is lower, the capillary water is completely consumed and self-desiccation takes place. For Portland cement, typical figures are 0.23–0.19 g/g for the chemically bound and physically bound (gel) water, respectively, and hence self-desiccation can be expected to occur in Portland cement systems with w/c below about 0.23 + 0.19 = 0.42 [40]. This number is expected to be significantly higher for CSA cements, see e.g. 0.75 g/g determined in [28]. According to our TGA measurements presented in the Supplementary Materials, Fig. S.2, the chemically bound water was around 0.38, 0.32 and 0.20 g/g of cement for the CSA, MIX and PC mortars, respectively. It should be noted that the sample preparation

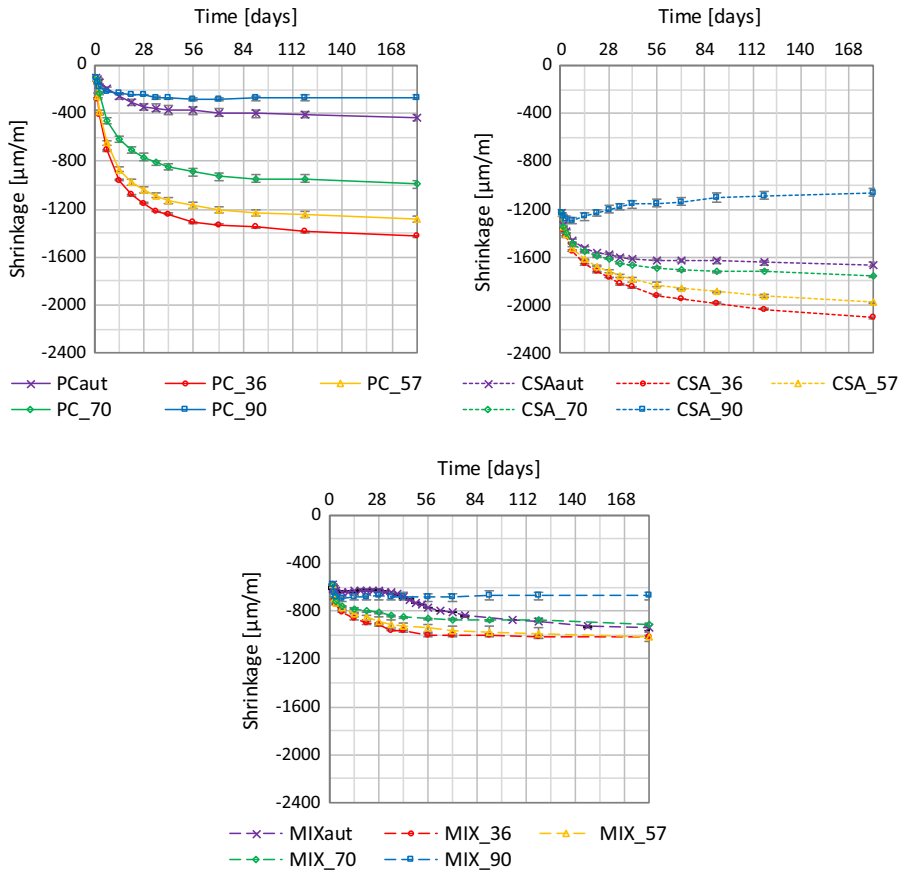

Fig. 6 Shrinkage evolution until 182 days as a combination of autogenous condition before 24 h and drying at different relative humidity after 24 h

protocol for TGA based on solvent exchange with isopropanol only allows resolving the chemically bound water but not the physically bound water. According to Hansen [41], all water confined in pores at RH below about 40% is physically bound water. Based on our DVS measurements we can conclude that the physically bound water is a couple of times higher for the CSA mortar than for the PC mortar (see e.g. values of water content retained at 10% RH in Fig. 2). These relatively high values of both chemically and physically bound water suggest that the w/c necessary for full hydration is significantly higher than the actual w/c of the mortars, i.e. 0.5 and 0.45 for the CSA and MIX systems, respectively.

At the same time, such relatively low w/c are necessary in order to produce stable mixes without segregation and with mechanical properties satisfying the practical requirements. The different w/c used for different mixes was motivated by the aim of obtaining mortars of similar mechanical properties at 28 d (particularly strength, see similar strength values at 28 d in Table 2) while maintaining constant volumetric content of cement paste (the actual component undergoing shrinkage).

The very fast kinetics of self-desiccation and autogenous shrinkage are in line with the calorimetry results presented in Fig. 1 (main peak visible at 2 h or 6 h for the CSA and MIX systems, respectively). As shown by the TGA results (see Supplementary Materials, Fig. S.1) a large part of the ettringite (the main hydration product of the CSA cement) was formed in these systems in the first 4 h of hydration.

The autogenous shrinkage results in Fig. 4 are in good agreement with the self-desiccation results in Fig. 3. CSA experienced the highest shrinkage. The peculiar shrinkage development of MIX, with a plateau after a few days, followed by renewed shrinkage after 28 days, closely follows the evolution of the internal RH. This trend is also in line with the TGA results presented in the Supplementary Materials (Fig. S.1). The initial fast formation of ettringite slows down after about 3 days and resumes in the second

phase after around 28 days. These results show that the shrinkage experienced by the systems containing the CSA is caused primarily by the self-desiccation resulting from binding large amounts of water by hydration products, mainly ettringite and aluminum hydroxide.

The rapid and high autogenous shrinkage reported here underlines the need for studying the early-age volume changes in the mixes prepared with CSA cements. In particular, the bi-modal shrinkage trend observed for the blended system should draw attention with regard to the risk of cracking also after the first few weeks after casting.

For the prismatic samples sealed with aluminum foil, practically no mass change is recorded during the investigated period, proving the effectiveness of sealing. On the contrary, in drying conditions the lower is the environmental RH, the higher the mass loss in time. The mass change evolution shown in Fig. 5 is in line with the internal RH of the samples. As expected, when the environmental RH is lower than the internal RH, some water evaporates and a mass loss is recorded. On the contrary, when the internal RH decreases due to self-desiccation below that of the curing environment, moisture is absorbed by the sample.

These considerations contribute to explain the mass gain in all mortars stored at 90% RH. For example, after an initial loss of mass during the first days, PC started to take up moisture from the external environment, partially compensating for the emptying of the pores due to self-desiccation. The point in time at which the mass gain started at 90% RH (after about 7 d) is also approximately in line with the moment when the internal RH in the mortars approached 90%, see Fig. 3. While PC started to gain mass after about 7 days, in CSA the internal RH (Fig. 3) rapidly dropped below the RH of the environment to which the samples were exposed already after 1 day and the samples gained mass immediately after opening. In MIX, the mass gain at 90% RH starts the latest (after more than one month), which is in line with its high internal RH in the first weeks and the onset of the second self-desiccation phase (see Fig. 3).

When the external RH is equal to or lower than 70%, all mixes experienced mass loss, indicating that the internal RH due to self-desiccation did not decrease below about 70% RH even at later times. The total amount of mass loss due to drying depends on two main factors: a) the size distribution of the pores manifested by the slope of the sorption isotherm (see Fig. 2) and b) the internal RH before drying starts. Considering factor a), the mass loss should be the highest for PC, which has in absolute terms steeper desorption isotherm than CSA and MIX mortars (0.025 g/g desorbed for PC between 90 and 30% RH compared to 0.022 g/g and 0.019 g/g, respectively).This is confirmed by the mass change measurements in Fig. 5. Considering factor b), CSA experienced the smallest mass change (see Fig. 5), since it reached the lowest RH due to self-desiccation. MIX falls in between the other two concretes. In MIX, the mass loss at the lowest RH was high due to the initially high RH at the onset of drying, but the differences between the different RH conditions are smaller than in PC, owing to the small slope of the sorption isotherm.

It should be also stressed that the overall mass change is affected not only by the moisture exchange due to water loss or gain, but also by the absorption of CO_2 from the atmosphere in the carbonation process [42]. The influence of the CO_2 on the mass change is generally ignored in standard drying shrinkage experiments. It can be avoided by drying in CO_2-free chambers/desiccators, which however prolongs and complicates the procedure and is only applicable to small/thin specimens [26, 43]. The mass gain due to carbonation is expected to be slower than the moisture loss, since part of the pores need to be first emptied of water to allow CO_2 ingress [44]. The interaction between drying and carbonation at early ages is complex, since both the reduced rate of cement hydration due to early drying (see [45]) and the internal RH [46] will also affect CO_2 binding. In general, the measured mass gain at high RH may be amplified by CO_2 absorption, while the moisture loss at low RH might be underestimated if this phenomenon is not considered. The quantification of the interaction between drying and carbonation, in particular for blends of CSA cement, requires further studies.

The observed volume changes of opened samples at high RH (90% RH) are in line with the above-discussed mass change results. In particular, expansion is observed whenever the internal RH is lower than the external RH and the sample absorbs moisture. The kinetics and the magnitude of this process in relation to the environmental RH are however more

complicated than the relationship between self-desiccation and autogenous shrinkage. This is because the drying process and corresponding shrinkage are not uniform in the whole sample. The gradients of moisture content, and therefore of RH and shrinkage strains in the sample exist from the moment when the sample is opened to drying (in opposition to the uniform distribution in autogenous conditions). As a result, the moisture and shrinkage profile is a combined effect of 1) the internal RH before opening of the sample to drying, 2) the external (ambient) RH, 3) the moisture transport (diffusion) in the sample, 4) the kinetics of self-desiccation and autogenous shrinkage ongoing in the core of the sample in parallel to the drying process. The overall measured shrinkage is further affected by the carbonation shrinkage [47]. In any case, the overall effect of drying at 90% RH was similar for all the samples: they all experienced a slight expansion compared to the autogenous shrinkage before opening. CSA and MIX had the smallest difference between the autogenous shrinkage and the overall shrinkage in drying conditions. In particular for CSA, it is evident that autogenous shrinkage is the main mechanism responsible for the overall shrinkage in this mortar, even when samples of small cross-Sect. (40-mm thickness) are measured.

An even larger contribution of autogenous shrinkage to the total deformation can be expected in real-size concrete members, where the effect of external drying (and carbonation shrinkage) is limited to a relatively thin surface zone [48]. In a recently published study on the same binder systems [33], autogenous shrinkage and drying shrinkage at 57% RH were measured on larger prismatic samples with dimensions 120 × 120 × 360 mm^3 starting at 1 day and up to 1 year. Despite the differences between mortars and concrete (in particular, the higher volume fraction of aggregate in the concrete that leads to smaller deformation) and the larger surface to volume ratio of the smaller mortar samples (about three times larger, resulting in faster drying of the mortars), the overall trends in mortars and concrete with the same binder are similar. The results on mortars presented in this new paper evidence the importance in mixtures with low w/b of measuring the very early deformations, from the time of final set. In fact, when measuring on concrete after 1 day PC shrinks more than CSA and CSA more than MIX. On the other hand, when the early rapid autogenous shrinkage of the mortars (between final setting time and 24 h) is considered, CSA shrinks more than the other two mortars. Also for MIX, the total deformations are considerably higher when considering the initial shrinkage in sealed conditions.

5 Conclusions

In this paper, the early-age shrinkage evolution for three mortars based on limestone Portland cement, CSA cement and a 50/50 blend of the two was investigated. To understand fully the early-age volume changes in real conditions, i.e. before and after demolding, a combination of autogenous and drying shrinkage was considered.

The investigation of the initial autogenous shrinkage underlined the strong tendency of the CSA-based systems to self-desiccate, evidencing their initial fast reaction and the high amount of water that is chemically bound by the cement. An especially interesting aspect of the initial severe self-desiccation is that the CSA-based systems experienced mass gain and swelling after being exposed to an environment at 90% RH.

In autogenous conditions, a particular situation was recorded for the blended mortar. Self-desiccation and autogenous shrinkage halted after a couple of days, but renewed self-desiccation and shrinkage occurred after about 1 month. This dual pattern of shrinkage appears to follow closely the internal RH evolution (self-desiccation). This is in line with the two stages of ettringite formation shown by the TGA.

This suggests that measuring autogenous shrinkage for a few weeks, as is usually done for Portland cement systems, may be too short for CSA-based blends.

The blended system showed the smallest shrinkage after 182 days but a mass change that is comparable to that of PC. This is probably linked to a microstructure characterized by large pores that lose large amounts of water without exerting significant pore pressure on the microstructure.

The comparison of shrinkage in sealed and in drying conditions shows that for mortars containing CSA, the overall shrinkage behavior is dominated by autogenous shrinkage even in relatively small samples (40-mm square cross-section) that are exposed to drying already at 1 d after casting. This further

underlines the need to focus on early-age phenomena when CSA binders are employed.

Acknowledgements We would like to thank EMPA laboratory group for their valued collaboration during the campaign organization. A special thanks to Nikolajs Toropovs for its contribution to the mechanical performance investigation campaign, to Frank Winnefeld for its valuable collaboration for the TGA data analysis and Luigi Brunetti for the support to the isothermal calorimetry test.

Funding Open Access funding provided by Lib4RI – Library for the Research Institutes within the ETH Domain: Eawag, Empa, PSI & WSL. The research presented in this paper, funded by the Swiss Federal Laboratories for Materials Science and Technology (Empa), was part of the PhD thesis of Davide Sirtoli, which was mainly funded by Italcementi S.p.A. Italcementi also provided the cements and the admixtures.

Compliance with ethical standards

Conflict of interest The authors declare that they have no conflict of interest.

References

1. Andrew RM (2018) Global CO2 emissions from cement production, 1928–2017. Earth Syst Sci Data. https://doi.org/10.5194/essd-10-2213-2018
2. Mohr SH, Wang J, Ellem G et al (2015) Projection of world fossil fuels by country. Fuel. https://doi.org/10.1016/j.fuel.2014.10.030
3. Juenger MCG, Winnefeld F, Provis JL, Ideker JH (2011) Advances in alternative cementitious binders. Cem Concr Res 41:1232–1243. https://doi.org/10.1016/j.cemconres.2010.11.012
4. Lothenbach B, Scrivener K, Hooton RD (2011) Supplementary cementitious materials. Cem Concr Res 41:1244–1256. https://doi.org/10.1016/j.cemconres.2010.12.001
5. Mokrzycki E, Uliasz-Bocheńczyk A (2003) Alternative fuels for the cement industry. Appl Energy 74:95–100. https://doi.org/10.1016/S0306-2619(02)00135-6
6. Mehta P (1980) Investigations on energy-saving cements. World Cem Technol 11:166–177
7. Gastaldi D, Boccaleri E, Canonico F, Bianchi M (2007) The use of Raman spectroscopy as a versatile characterization tool for calcium sulphoaluminate cements: a compositional and hydration study. J Mater Sci 42:8426–8432. https://doi.org/10.1007/s10853-007-1790-8
8. Zhang L, Glasser FP (2002) Hydration of calcium sulfoaluminate cement at less than 24 h. Adv Cem Res 14:141–155. https://doi.org/10.1680/adcr.2002.14.4.141
9. Lura P, Winnefeld F, Klemm S (2010) Simultaneous measurements of heat of hydration and chemical shrinkage on hardening cement pastes. J Therm Anal Calorim 101:925–932. https://doi.org/10.1007/s10973-009-0586-2
10. Janotka I, Krajči L (1999) An experimental study on the upgrade of sulfoaluminate—belite cement systems by blending with Portland cement. Adv Cem Res 11:35–41. https://doi.org/10.1680/adcr.1999.11.1.35
11. Pelletier L, Winnefeld F, Lothenbach B (2010) The ternary system Portland cement-calcium sulphoaluminate clinker-anhydrite: hydration mechanism and mortar properties. Cem Concr Compos 32:497–507. https://doi.org/10.1016/j.cemconcomp.2010.03.010
12. Lan W, Glasser FP (1996) Hydration of calcium sulphoaluminate cements. Adv Cem Res 8:127–134
13. Chen IA, Hargis CW, Juenger MCG (2012) Understanding expansion in calcium sulfoaluminate-belite cements. Cem Concr Res 42:51–60. https://doi.org/10.1016/j.cemconres.2011.07.010
14. Marchi M, Costa U (2011) Influence of the calcium sulphate and W/C ratio on the hydration of calcium sulfoaluminate cement. In: 13th international congress chemistry cement, 1–7
15. Winnefeld F, Barlag S (2009) Influence of calcium sulfate and calcium hydroxide on the hydration of calcium sulfoaluminate clinker. ZKG Int 62:42–53
16. Meddah MS, Suzuki M, Sato R (2011) Influence of a combination of expansive and shrinkage-reducing admixture on autogenous deformation and self-stress of silica fume high-performance concrete. Constr Build Mater 25:239–250. https://doi.org/10.1016/j.conbuildmat.2010.06.033
17. Slatnick S, Riding KA, Folliard KJ et al (2011) Evaluation of autogenous deformation of concrete at early ages. ACI Mater J 108:21–28. https://doi.org/10.14359/51664212
18. Noguchi T, Sun-Gyu P, Maruyama I (2005) Mechanical properties of high-performance concrete with expansive additive and shrinkage reducing admixtures under simulated completely-restrained condition at early age. In: Self-desiccation and its importance in concrete technology: proceedings of the 4th international seminar
19. Wyrzykowski M, Terrasi G, Lura P (2018) Expansive high-performance concrete for chemical-prestress applications. Cem Concr Res. https://doi.org/10.1016/j.cemconres.2018.02.018
20. Le-Bihan T, Georgin JF, Michel M et al (2012) Measurements and modeling of cement base materials deformation at early age: the case of sulfo-aluminous cement. Cem

Concr Res 42:1055–1065. https://doi.org/10.1016/j.cemconres.2012.04.004
21. Péra J, Ambroise J (2004) New applications of calcium sulfoaluminate cement. Cem Concr Res 34:671–676. https://doi.org/10.1016/j.cemconres.2003.10.019
22. Ambroise J, Péra J (2009) Use of calcium sulfoaluminate cement to improve strength of mortars at low temperature. Concr Repair Rehabil Retroffit II:881–886
23. Quillin K (2001) Performance of belite-sulfoaluminate cements. Cem Concr Res 31:1341–1349. https://doi.org/10.1016/S0008-8846(01)00543-9
24. Zhang L, Su M, Wang Y (1999) Development of the use of sulfo- and ferroaluminate cements in China. Adv Cem Res 11:15–21. https://doi.org/10.1680/adcr.1999.11.1.15
25. Bentur A (2003) Evaluation of early age cracking characteristics in cementitious systems. Mater Struct 36:183–190. https://doi.org/10.1617/14014
26. Weiss J, Lura P, Rajabipour F, Sant G (2008) Performance of shrinkage-reducing admixtures at different humidities and at early ages. ACI Mater J. https://doi.org/10.14359/19977
27. Mejlhede Jensen O, Freiesleben Hansen P (1996) Autogenous deformation and change of the relative humidity in silica fume-modified cement paste. ACI Mater J. 93:539–543. https://doi.org/10.14359/9859
28. Lura P, Winnefeld F, Fang X (2015) A simple method for determining the total amount of physically and chemically bound water of different cements. J Therm Anal Calorim 130(2):653–660
29. Zhang P, Wittmann FH, Zhao TJ et al (2011) Neutron radiography, a powerful method to determine time-dependent moisture distributions in concrete. Nucl Eng Des 241(12):4758–476629
30. Igarashi SI, Bentur A, Kovler K (2000) Autogenous shrinkage and induced restraining stresses in high-strength concretes. Cem Concr Res 30:1701–1707. https://doi.org/10.1016/S0008-8846(00)00399-9
31. Lura P, Van Breugel K, Maruyama I (2001) Effect of curing temperature and type of cement on early-age shrinkage of high-performance concrete. Cem Concr Res 31:1867–1872. https://doi.org/10.1016/S0008-8846(01)00601-9
32. Neithalath N, Pease B, Moon JH et al (2005) Considering moisture gradient and time-dependent crack growth in restrained concrete elements subjected to drying. NSF Work High Perform Concr, pp 279–290
33. Sirtoli D, Riva P, Tortelli S, Marchi M (2016) Mechanical performance of sulpho-based rapid hardening concrete. In: The new boundaries of structural concrete. Session C—New scenarios for concrete33
34. Sirtoli D, Wyrzykowski M, Riva P et al (2019) Shrinkage and creep of high-performance concrete based on calcium sulfoaluminate cement. Cem Concr Compos 98:61–73. https://doi.org/10.1016/j.cemconcomp.2019.02.006
35. BS EN 12390-13 (2013) Testing hardened concrete—part 13: determination of secant modulus of elasticity in compression. BSI—Br Stand Inst
36. Guimarães D, Oliveira VDA, Leão VA (2016) Kinetic and thermal decomposition of ettringite synthesized from aqueous solutions. J Therm Anal Calorim. https://doi.org/10.1007/s10973-016-5259-3
37. ASTM Standard (2009) C1698–09 Test method for autogenous strain of cement paste and mortar
38. Wyrzykowski M, Hu Z, Ghourchian S et al (2017) Corrugated tube protocol for autogenous shrinkage measurements: review and statistical assessment. Mater Struct 50:57. https://doi.org/10.1617/s11527-016-0933-2
39. Powers TC, Brownyard TL (1946) Studies of the physical properties of hardened Portland cement paste. In: Journal Proceedings, pp 101–132
40. Jensen OM, Hansen PF (2001) Water-entrained cement-based materials—I. Cem Concr Res, Principles and theoretical background. https://doi.org/10.1016/S0008-8846(01)00463-X
41. Hansen TC (1986) Physical structure of hardened cement paste. Mater Struct, A classical approach. https://doi.org/10.1007/BF02472146
42. Pade C, Guimaraes M (2007) The CO2 uptake of concrete in a 100 year perspective. Cem Concr Res. https://doi.org/10.1016/j.cemconres.2007.06.009
43. Di Bella C, Wyrzykowski M, Griffa M et al (2015) Application of microstructurally-designed mortars for studying early-age properties: microstructure and mechanical properties. Cem Concr Res. https://doi.org/10.1016/j.cemconres.2015.08.001
44. Leemann A, Loser R, Münch B, Lura P (2017) Steady-state O2 and CO2 diffusion in carbonated mortars produced with blended cements. Mater Struct Constr. https://doi.org/10.1617/s11527-017-1118-3
45. Wyrzykowski M, Lura P (2016) Effect of relative humidity decrease due to self-desiccation on the hydration kinetics of cement. Cem Concr Res 85:75–81. https://doi.org/10.1016/j.cemconres.2016.04.003
46. Wierig H (1984) Longtime studies on the carbonation of concrete under normal outdoor exposure. Hann Univ, Proc RILEM
47. Chen JJ, Thomas JJ, Jennings HM (2006) Decalcification shrinkage of cement paste. Cem Concr Res. https://doi.org/10.1016/j.cemconres.2005.11.003
48. Kovler K, Zhutovsky S (2006) Overview and future trends of shrinkage research. In: Materials and structures/materiaux et constructions